Non-steady-state photoelectromotive-force generation in an interferometer with optoelectronic feedback

Mikhail Bryushinin* and Igor Sokolov
A. F. Ioffe Physical Technical Institute, 194021, St. Petersburg, Russia
(Received 15 November 2007; published 5 March 2008)

The generation of optical phase oscillations is investigated in an interferometer using a $Bi_{12}SiO_{20}$ non-steady-state photoelectromotive-force detector. Phase modulation of the signal optical beam is created by the detected signal itself, in contrast to the standard forced regime where such modulation is produced by an external source. The conditions necessary for the self-excitation of the oscillations are obtained using the results of the small-signal approach for the non-steady-state photoelectromotive-force effect. The amplitude and frequency of the oscillations are defined by the photoelectric properties of the detector but not by the feedback loop. The dependencies of the oscillations on the time and gain factor are measured for both the diffusion and drift regimes.

DOI: 10.1103/PhysRevA.77.033809 PACS number(s): 42.65.Sf, 42.70.Nq

I. INTRODUCTION

Among the nonlinear phenomena observed in photorefractive crystals, there are effects whose appearance or specific behavior is determined by an additional feedback loop. Stabilization of a holographic setup was one of the earliest and the most important applications of optoelectronic feedback [1]. It is implemented using a detection scheme and a piezoelectric mirror placed in one of the arms of the setup. The mirror is driven by the amplified voltage of the detector providing the necessary feedback loop. Such feedback keeps the difference of the optical path lengths constant and correspondingly stabilizes the position of the interference fringes. As a result the holograms are recorded with a high modulation index.

Further investigations of feedback operations have revealed dramatic changes in photorefractive recording itself. It was found that self-stabilized recording in $LiNbO_3$ leads to an almost 100% diffraction efficiency of the hologram [2,3]. It was shown later that this regime is a quasi-steady-state: the diffraction efficiency oscillates in the close vicinity of 1 (or 0) and the phase of the controlled beam grows almost linearly [4,5]. These effects are accompanied by light scattering reduction [6] and fringe bending [4]. In addition, the feedback-controlled two-wave coupling can result in the excitation of space charge waves [7]. A number of nonlinear oscillation regimes is predicted in Ref. [8] for materials with local and nonlocal photorefractive responses and different phase relations between the diffracted and transmitted beams.

Generally speaking, the implementation of feedback in optical schemes reveals features typical of those in common dynamical systems (mechanical, electronic, biological) considered in the theory of oscillations and control theory [9,10]. For example, the negative feedback in a Michelson interferometer provides the ability to linearize the sensor (photodiode) output, allowing detection of large displacements [11]. The conventional electronic operational amplifier demonstrates similar behavior with a feedback loop. Various optical schemes with positive feedback, such as lasers, molecular cells inside a Fabry-Pérot resonator, and hybrid schemes with birefringent materials [12], reveal oscillatory or bistable behavior which also has analogs in electronics and mechanics (harmonic oscillators, triggers). Since the presence of properly chosen feedback in a dynamical system not only improves its performance but can also provide observation of new nonlinear phenomena, we have applied the feedback operation concept to a sensor based on the effect of the non-steady-state photoelectromotive force.

The non-steady-state photoelectromotive force (photo-EMF) is a holography-related effect and it appears in a semiconductor material illuminated by an oscillating light pattern. Such illumination is usually created by two coherent light beams, one of which is phase modulated with frequency ω. The alternating current results from the periodic relative shifts of the photoconductivity and space charge gratings which arise in the crystal volume under illumination. Like holographic recording in photorefractive crystals, this effect demonstrates adaptive properties that promote its application in such areas as vibration monitoring, velocimetry, etc. [13]. In contrast to holographic methods, this technique allows the direct transformation of phase-modulated optical signals into electrical current and can be applied for characterization of centrosymmetrical and even amorphous materials. Since the photocurrent originates from the interaction of both the photoconductivity and the space charge gratings, a lot of photoelectric parameters can be measured [14].

In this study we introduce positive feedback and organize the generation mode operation in the interferometer using a non-steady-state photo-EMF detector (Fig. 1). In contrast to techniques developed in Refs. [1–7] we do not use any dither signals and synchronous detection. Our approach implies the utilization of a conventional wideband amplifier in the electronic circuit. Both the diffusion and drift regimes are investigated theoretically and experimentally in a $Bi_{12}SiO_{20}$ crystal.

II. THEORETICAL ANALYSIS

Let us start the analysis of our interferometric scheme [Fig. 1(a)] with formulation of the problem in terms of os-

*mb@mail.ioffe.ru

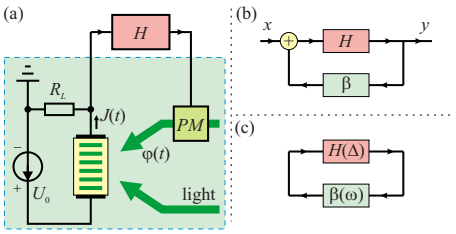

FIG. 1. (Color online) Block diagrams illustrating closed-loop operation of the interferometric scheme studied in this paper (a); general feedback structure (b); and general oscillator scheme (c). PM is the phase modulator.

cillation and control theory [9–11]. Dynamical systems are often represented by block diagrams, which have a unique algebra and set of transformations. The block diagrams are used because they are a shorthand pictorial representation of the cause-and-effect relationship between the input and output in a real system, and they are a convenient method for characterizing the functional relationships between components. One important arrangement is the general feedback form illustrated in Fig. 1(b). In this figure, H and β represent the transfer functions from the input to the output of the systems contained within their respective boxes. The overall transfer function is as follows:

$$T = \frac{H}{1 - H\beta}. \tag{1}$$

The product $H\beta$ is often called the loop gain. When this product tends to unity, the transfer function diverges, which corresponds to the appearance of an instability and unlimited growth of oscillations in a closed-loop system.

The basic form of a harmonic oscillator is an amplifier with the output attached to a narrowband filter $[\beta=\beta(\omega)]$, and the output of the filter attached back to the input of the amplifier [Fig. 1(c)]. The unlimited growth of oscillations is usually restricted by nonlinearity of the amplifier observed at large amplitudes, i.e., $H=H(\Delta)$. The relation

$$H(\Delta)\beta(\omega) = 1 \tag{2}$$

is the main equation (Barkhausen equation) defining the amplitude Δ_g and frequency ω_g in the steady-state oscillation regime. So, our main goal in this section is to obtain the analogous equation for the interferometric scheme using the non-steady-state photo-EMF detector and feedback loop [Fig. 1(a)] and calculate the corresponding oscillation amplitudes and frequencies.

Let us assume the crystal is illuminated by an oscillating interference pattern created by two light beams, one of which is phase modulated with amplitude Δ and frequency ω:

$$I(x,t) = I_0[1 + m\cos(Kx + \Delta\cos\omega t)]. \tag{3}$$

Here I_0 is the average intensity, m and K are the contrast and spatial frequency of the interference pattern, and Δ and ω are the amplitude and frequency of the phase modulation.

Such illumination excites an ac current in the crystal volume via the non-steady-state photo-EMF effect. This current produces a corresponding voltage at the load resistor, which is then amplified and transferred into a phase modulation with amplitude Δ using the electro-optic modulator:

$$\Delta = \frac{JR_L H}{U_\pi/\pi}, \tag{4}$$

where U_π is the half-wave voltage of the phase modulator, R_L is the load resistance, and H is the gain factor of the amplifier. So the feedback loop is closed.

We can easily rewrite Eq. (4) in a form analogous to the Barkhausen equation (2):

$$H\left(\pi\frac{J^\omega(\omega,\Delta)R_L}{U_\pi\Delta}\right) = 1, \tag{5}$$

where J^ω is the complex amplitude of the photo-EMF signal in the small-signal approximation. As seen, the expression in parentheses plays the role of the feedback transfer function β in the standard Barkhausen equation (2).

We shall consider the ideal amplifier with a flat frequency transfer function and infinite dynamic range:

$$H = \text{const}(\omega, U_{in}). \tag{6}$$

In this case the frequency and amplitude of oscillations are defined by the frequency response and nonlinearity of the non-steady-state photo-EMF but not by the amplifier.

There are two different basic mechanisms of space charge formation—diffusion and drift [15]. Let us proceed with analysis of the former.

A. Diffusion mechanism of recording

For the diffusion mechanism of recording, no external voltage is applied to the sample and the amplitude of the non-steady-state photocurrent excited in the crystal with electron conductivity is given by the following expression [14,16]:

$$J^\omega = \frac{-Sm^2 J_0(\Delta)J_1(\Delta)\sigma_0 E_D i\omega\tau_M}{1 - \omega^2\tau\tau_M + i\omega[\tau + \tau_M(1 + K^2L_D^2)]}; \tag{7}$$

where S is the electrode area, σ_0 is the average photoconductivity of the sample, E_D is the diffusion field, τ_M is the Maxwell relaxation time, τ is the relaxation time of the conductivity, L_D is the diffusion length of electrons, and $J_n(\Delta)$ is the Bessel function of the first kind of nth order.

First let us consider the case of a real gain factor

$$H = H_r \tag{8}$$

and

$$\text{Im}(H_r) = 0. \tag{9}$$

This situation is typical for conventional analog wideband amplifiers.

The phase conditions, i.e., phase shifts of the amplifier and feedback, define the operating frequency of generators in oscillation theory; namely, the sum of amplifier and feedback

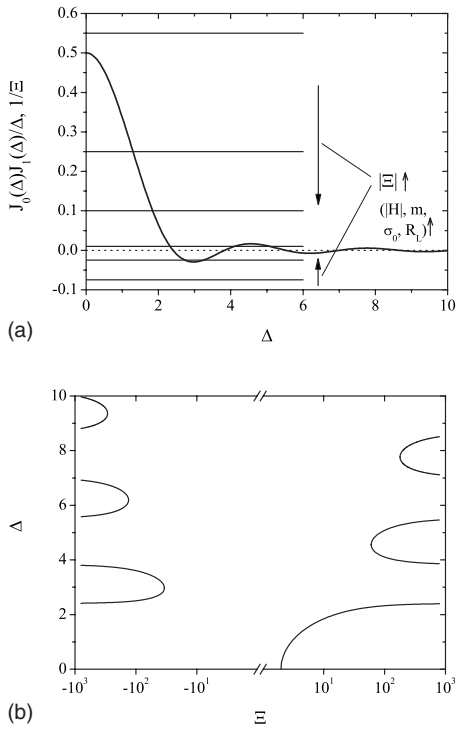

FIG. 2. Graphic solution of Eq. (11) and corresponding dependence of the oscillation amplitude on the normalized gain factor.

phase shifts must be a multiple of 2π. We can always set the phase of Δ to zero by the appropriate choice of the time origin. As follows from Eq. (7) the complex amplitude of the photocurrent is a real value for modulation frequency equal to

$$\omega_g = \omega_m = (\tau\tau_M)^{-1/2}. \tag{10}$$

It corresponds to the maximum in the frequency dependence of the photo-EMF amplitude.

The amplitude of oscillations in the conventional generators (electrical, optical, etc.) is usually defined by the amplifier's nonlinearity originating for large amplitudes. In our case the saturation of the non-steady-state photo-EMF for large Δ will confine the generation amplitude. As follows from Eqs. (5) and (7) it is defined as

$$J_0(\Delta)J_1(\Delta)/\Delta = 1/\Xi. \tag{11}$$

Here we introduced the dimensionless gain factor Ξ:

$$\Xi = -\xi H_r E_D, \tag{12}$$

$$\xi = \frac{\pi S m^2 \sigma_0 R_L}{U_\pi (1 + K^2 L_D^2)}. \tag{13}$$

Equation (11) is nonlinear and can be solved graphically or numerically (Fig. 2). The oscillation with lowest amplitude occurs when the dimensionless gain factor Ξ is positive and reaches 2, i.e., $\Xi > 2$ (Fig. 2). Increasing the gain factor from this value, one can magnify the oscillation amplitude up to $\Delta \simeq 2.4$. When the gain factor reaches $\Xi \simeq 60$, 180, etc. oscillations with higher amplitudes ($\Delta \simeq 4.6$, 7.8, etc.) become possible as well. As seen, each of these higher modes splits into two submodes with higher and lower amplitudes. Another feature is also seen from Fig. 2. The first mode (with lowest amplitude) is characterized by the soft regime of generation, i.e., such generation can appear as the result of a very small deviation from the unstable equilibrium $\Delta = 0$ (e.g., from the noise of the load resistor). Higher modes are characterized by a hard regime of generation and require sufficient initial deviation, which should be of the order of the oscillation amplitude, i.e., ~4.6, 7.8, etc.

Generation is also possible for negative gain factors $\Xi < 0$ (Fig. 2). In this case the oscillations with lowest amplitude $\Delta \simeq 3.0$ appear when the gain factor reaches $\Xi \simeq -34$. The behavior of the modes is analogous to that for positive gain factors. All the modes are characterized by a hard regime of generation.

Now let us suppose that the amplifier of the photo-EMF signal both increases the amplitude and introduces a $\pi/4$ phase shift:

$$H = H_r \exp(i\pi/4). \tag{14}$$

Then the generation frequency equals

$$\omega_g = \omega_1 = \tau_{sc}^{-1} = [\tau_M(1 + K^2 L_D^2)]^{-1}. \tag{15}$$

It should be noticed that this estimation is obtained for the condition $\tau \ll \tau_M$, which is typical for highly resistive semiconductors (e.g., for photorefractive $Bi_{12}SiO_{20}$). The frequency ω_1 is the first cutoff frequency of the non-steady-state photo-EMF for the case of forced excitation of the signal [14] and it is the inverse of the space charge formation time τ_{sc} [15].

The amplitude of oscillation is calculated from Eq. (11) with

$$\Xi = -\xi H_r E_D/\sqrt{2}. \tag{16}$$

The coefficient $\sqrt{2}$ appears here because the photo-EMF amplitude at frequency ω_1 is $\sqrt{2}$ times lower than that at frequency ω_m. Since the amplitude of oscillations Δ is defined from the same equation as for the case of real H, its behavior with respect to the gain factor Ξ should be analogous to that described above.

Finally, let the gain factor equal

$$H = H_r \exp(-i\pi/4). \tag{17}$$

Then the oscillation frequency corresponds to the second cutoff frequency of the photo-EMF signal:

$$\omega = \omega_2 = (1 + K^2 L_D^2)/\tau \tag{18}$$

and the amplitude is deduced from Eqs. (11) and (16).

B. Drift mechanism of recording

In this case an external dc electric field E_0 is applied to the crystal and the photo-EMF amplitude is defined by the following expression [16]:

$$J^{\omega} = \frac{0.5Sm^2J_0(\Delta)J_1(\Delta)\sigma_0[i2E_0 - \omega\tau_M(E_0 + iE_D)]}{1 - \omega^2\tau\tau_M + i\omega[\tau + \tau_M(1 + K^2L_D^2 + iKL_0)]} - \frac{0.5Sm^2J_0(\Delta)J_1(\Delta)\sigma_0[i2E_0 - \omega\tau_M(E_0 - iE_D)]}{1 - \omega^2\tau\tau_M + i\omega[\tau + \tau_M(1 + K^2L_D^2 - iKL_0)]}. \quad (19)$$

First let us suppose the gain factor is real [Eqs. (8) and (9)]. In addition, let us consider the case of rather large electric fields such that the conditions $E_0 \gg E_D$, $KL_0 \gg 1 + K^2L_D^2$ are satisfied. Then the generation frequency is equal to the first resonant frequency of the non-steady-state photo-EMF excited in the forced regime [16] and it is equal to the frequency of the space charge wave (trap-recharging wave)—one of the fundamental modes of the space charge oscillation in semiconductors [15]:

$$\omega_g = \omega_{r1} = \omega_{\text{scw}} = (\tau_M KL_0)^{-1}. \quad (20)$$

The amplitude of oscillations is deduced from Eq. (11) with

$$\Xi = \xi H_r E_0 KL_0. \quad (21)$$

As follows from Eqs. (12) and (21) the generation mode is achieved more easily in the drift regime, namely, the required gain factor of the amplifier H is E_0KL_0/E_D times smaller than that for the diffusion regime. This is because of the effect of the resonant amplification of the running space charge gratings in an external dc field. Moreover, the sign of the non-steady-state photo-EMF signal in the diffusion and drift regimes differs by π, so the necessary phase shifts of the amplifier are opposite for these cases.

Now let us assume the gain factor is purely imaginary:

$$H = H_r \exp(i\pi/2). \quad (22)$$

Then generation frequency equals

$$\omega_g = \omega_{r2} = \omega_{dw} = K\mu E_0. \quad (23)$$

The frequency ω_{r2} is the second resonant frequency of the non-steady-state photo-EMF effect [16], and it is equal to the frequency of another eigenmode of space charge oscillations—the drift wave [17]. The amplitude of oscillations is deduced from Eq. (11) with

$$\Xi = \xi H_r E_0/2. \quad (24)$$

In this section we considered theoretically the self-excitation regime for the non-steady-state photo-EMF effect. The results of the analysis shows the possibility of materials characterization using this technique. Indeed, the generation frequency is defined by the characteristic times of space charge and conductivity relaxation. In contrast to the forced regime of signal excitation, the considered technique does not require measurements of the frequency transfer function; the oscillation frequency can be measured by a conventional frequency counter.

III. EXPERIMENTAL ARRANGEMENT

The scheme of the experimental arrangement is presented in Fig. 3. The second harmonic of a neodymium-doped yttrium aluminum garnet (Nd:YAG) laser is used as the source of the coherent radiation ($\lambda = 532$ nm, $P_{\text{out}} \simeq 20$ mW). The light is split into two beams. One of them is phase modulated by an electro-optic modulator (the light is passed twice through the modulator to increase the efficiency of modulation, $U_\pi = 193$ V). Then these two beams are directed onto the crystal's surface, where they produce an oscillating interference pattern with the following parameters: $I_0 = 0.75$ W/cm^2, $m = 0.95$, $K = 1.0$ μm^{-1} for the diffusion regime of signal excitation and $I_0 = 0.10$ W/cm^2, $m = 0.17$, $K = 0.16$ μm^{-1} for the drift regime. The current arising in the crystal under such illumination produces a voltage on the load resistor ($R_L = 110$ and 10 kΩ for the diffusion and drift mechanisms of signal excitation, respectively). Then this voltage is amplified, measured by the analog-to-digital converter connected to the computer, and applied back to the electro-optic modulator. The amplifier is characterized by the gain factor 40–80 dB, phases 0 and π, flat frequency response in the range 1.5 Hz–150 kHz, and highest output voltage of 100 V. In our experiments we used a conventional undoped $Bi_{12}SiO_{20}$ crystal. The sample has the following dimensions: $10 \times 4 \times 1$ mm^3. The silver paste electrodes (3×3 mm^2) are painted on the lateral surfaces. The interelectrode spacing equals $L = 1$ mm. For the realization of the drift regime of signal excitation an external dc voltage was applied to the crystal.

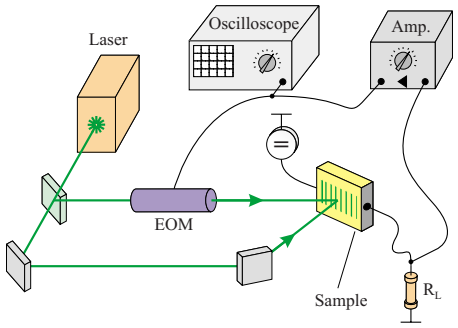

FIG. 3. (Color online) Simplified scheme of the experimental setup. EOM is the electro-optic modulator; Amp is the wideband amplifier with regulated gain factor.

IV. EXPERIMENTAL RESULTS

First we carried out standard measurements of the non-steady-state photo-EMF in a $Bi_{12}SiO_{20}$ crystal. These experiments help us to find the necessary conditions for realization of the self-excitation regime and analyze it. Frequency transfer functions of the non-steady-state photo-EMF are presented in Fig. 4. The dependencies were measured for zero external electric field (diffusion regime of signal excitation) and a rather large field of 10 kV/cm (drift regime). We have approximated them by Eqs. (7) and (19). The frequency of the maximum is one of the fitting parameters. The photocurrent is also characterized by a phase shift equal to π (diffusion regime) and 0 (drift regime) at this frequency. It was found to be $\omega_m/2\pi = 5.9$ kHz (for $E_0 = 0$) and $\omega_m/2\pi = 120$ Hz (for $E_0 = 10$ kV/cm). That is, these values are ex-

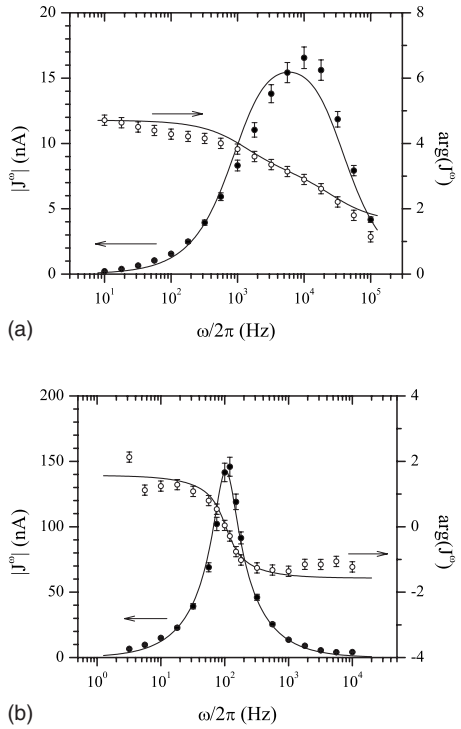

FIG. 4. Amplitude and phase frequency transfer functions of the non-steady-state photo-EMF measured in $Bi_{12}SiO_{20}$ crystal at $E_0=0$ (top figure, $\Delta=0.16$) and 10 kV/cm (bottom figure, $\Delta=0.32$).

pected to be the generation frequencies in experiments with positive feedback.

When a feedback loop with appropriate phase shift and gain factor is created, oscillations of the current in the crystal and oscillations of the optical phase of the signal beam arise. The minimum gain factors are the following: $H\simeq -6.0\times 10^3$ for the diffusion regime of the signal excitation and $H\simeq 1.4\times 10^4$ for the drift one. Let us calculate the corresponding theoretical values using the material parameters from Ref. [18]: $sN_D=1.06\times 10^{20}$ $J^{-1}\,m^{-1}$ and $\mu/(\gamma N_A)=6.38\times 10^{-11}$ $m^2\,V^{-1}$. Assuming the illuminated electrode area to be $S=3$ mm^2 (unexpanded beams, $E_0=0$) and $S=9$ mm^2 (expanded beams, $E_0=10$ kV/cm) we obtain the following estimations: $H=-5.2\times 10^3$ for the diffusion and

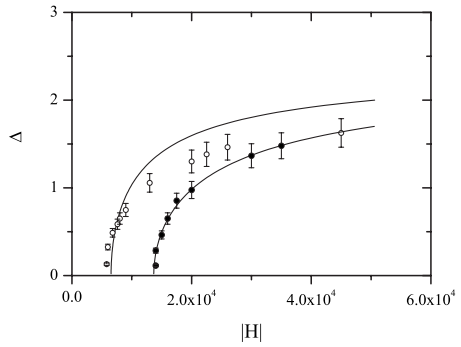

FIG. 5. Dependencies of the phase oscillation amplitude on the gain factor of the amplifier measured in $Bi_{12}SiO_{20}$ crystal at $E_0=0$ (open circles) and 10 kV/cm (filled circles).

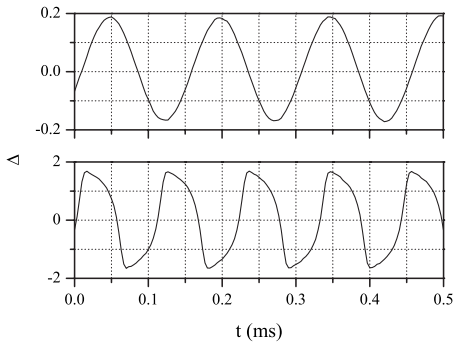

FIG. 6. Light phase oscillations measured in $Bi_{12}SiO_{20}$ crystal for $E_0=0$ and for two gain factors of the amplifier: $H=-6.0\times 10^3$ (top figure) and -4.5×10^4 (bottom figure).

4.5×10^3 for the drift regime. One can note the good coincidence of the experimental and theoretical values for the former case and the rather passable agreement for the latter. We suppose the discrepancy obtained for the case $E_0\neq 0$ can be attributed to the voltage drop on the blocking contact reducing the electric field in the crystal volume and to space charge grating saturation effects.

We measured the dependencies of the optical phase oscillation amplitude on the gain factor of the voltage amplifier (Fig. 5). We note the following peculiarity. When the oscillations appear, they have rather small amplitude. In addition we observed no hysteresis effect, i.e., oscillations arise and disappear at the same gain factor values. So we can state that the constructed optoelectronic generator is characterized by a "soft" regime of excitation. The experimental dependencies were approximated by Eq. (11).

Let us consider the time dependencies of the oscillations (Figs. 6 and 7). They were measured for the diffusion and drift regimes of photo-EMF excitation and for two values of the gain factor: one is near the excitation threshold and other is the maximum value where linear properties of the amplifier are guaranteed. Note that oscillations are sinusoidal for the case of small gain factors. Their amplitude is rather small and the frequency corresponds well to the frequency of the current maximum in experiments with forced excitation of the non-steady-state photo-EMF signal: $\omega_g/2\pi=6.7$ kHz (for $E_0=0$, $H=6.0\times 10^3$) and $\omega_g/2\pi=106$ Hz (for E_0

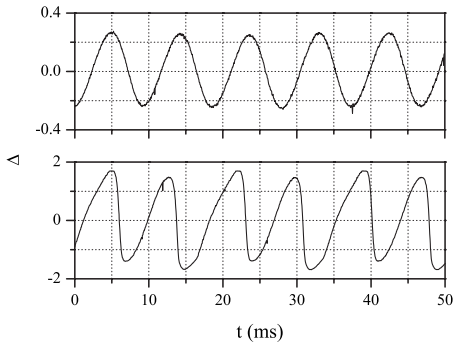

FIG. 7. Light phase oscillations measured in $Bi_{12}SiO_{20}$ crystal at $E_0=10$ kV/cm and for two gain factors: $H=1.4\times 10^4$ (top figure) and 3.5×10^4 (bottom figure).

$=10$ kV/cm, $H=1.4\times10^4$). When the gain factor increases the oscillations become nonharmonic and their frequency increases: $\omega_g/2\pi=9.1$ kHz (for $E_0=0$, $H=4.5\times10^4$) and $\omega_g/2\pi=117$ Hz (for $E_0=10$ kV/cm, $H=3.5\times10^4$). We noticed an important feature: the deviation of the generation frequency in the diffusion regime is larger than the deviation in the drift regime for comparable increase of the gain factor. This is most probably due to the resonant nature of the signal excitation in the drift regime. It should be noted that the observed time dependencies demonstrated instability for certain gain factors. For low gain factors, instability is associated with fluctuations in the experimental environment (instabilities of the laser power and external voltage, vibrations, etc.). In the drift regime and for large gain factors, subharmonics with frequencies $\omega_g/2$ and $\omega_g/3$ appear and disappear during measurements (Fig. 7). This feature can be associated with the effects of space charge wave instability described earlier [19,20].

The possibility for measurements of photoelectric parameters was pointed out in Sec. II. As follows from Eq. (10), the product $\tau\tau_M=5.6\times10^{-10}$ s^2 can be evaluated directly from the oscillation frequency in the diffusion regime of recording ($E_0=0$). For the drift regime of signal excitation ($E_0=10$ kV/cm) the oscillation frequency exactly equals the eigenfrequency of the space charge waves, i.e., $\omega_{sc}=670$ s^{-1}.

V. DISCUSSION

In this paper we have studied an interferometer regime using a detector based on the non-steady-state photo-EMF effect. That is, oscillations of the optical phase are generated in an interferometer with a $Bi_{12}SiO_{20}$ detector and an optoelectronic feedback loop. The main parameters of such oscillations, i.e., amplitude and frequency, are defined mainly by the nonlinearity of the amplitude characteristic of the non-steady-state photo-EMF effect and the photoelectric properties of the crystal, and not by the experimental environment. This feature can be used for semiconductor testing applications. For example, the frequency of the oscillations excited in the drift regime of recording equals the eigenfrequency of the space charge waves—the fundamental mode of the space charge oscillations. Using this technique, we have estimated this eigenfrequency along with another complex parameter—the product $\tau\tau_M$. Determination of the basic parameters like the Maxwell relaxation time τ_M, photoconductivity relaxation time τ, and carrier mobility μ (Sec. II) requires a wideband electronic amplifier with phase shifts $\pm\pi/4$ and $\pi/2$. Unfortunately we did not find an analog scheme of such a device. Nevertheless, there is the possibility to construct the amplifier with a digital filter providing the necessary phase shift via direct fast Fourier transform (FFT), multiplication by the desired transfer function, and inverse FFT. Nowadays semiconductor manufacturers offer digital signal processors that perform a 256-point FFT for ~1 μs [21]. So a filter frequency bandwidth of ~100 kHz is expected, and it would be quite enough for the experiments. We consider such experimental work as a task for the future, when these technologies will be more accessible.

The technique developed can also be applied for the detection of phase-modulated optical signals, e.g., in laser ultrasonics. One can realize the regenerative principle of signal amplification in the considered interferometric scheme with feedback loop. In this case one of the interfering laser beams [Fig. 1(a)] should carry the information signal (e.g., from a vibrating object), and the dimensionless gain factor Ξ should be chosen slightly smaller than the critical value ($\Xi<2$). The amplitude of the detected photo-EMF signal can be increased several times with respect to the standard scheme [13] (as a rule, the reachable magnification factor is defined by the stability of the components of the setup).

The analysis of the considered phenomenon is based on the linear approach of the non-steady-state photo-EMF theory. It allowed us to describe the rise of the generation regime when the amplitude of the oscillations is small enough. However, some peculiarities observed in the experiments, e.g., frequency shift, nonharmonic form of the oscillations with large amplitude, and subharmonic generation, show the necessity of a more detailed theoretical analysis of the effect.

ACKNOWLEDGMENTS

Support from INTAS (Project No. 04-78-7227), from the President of the Russian Federation (Grant No. NSh-5596.2006.2), from the Russian Foundation for Basic Research (Grants No. 07-02-01099 and No. 05-02-17775), and from the Russian Science Support Foundation is gratefully acknowledged.

[1] A. A. Kamshilin, J. Frejlich, and L. Cescato, Appl. Opt. **25**, 2375 (1986).
[2] A. A. Freschi and J. Frejlich, J. Opt. Soc. Am. B **11**, 1837 (1994).
[3] P. M. Garcia, K. Buse, D. Kip, and J. Frejlich, Opt. Commun. **117**, 235 (1995).
[4] V. P. Kamenov, K. H. Ringhofer, B. I. Sturman, and J. Frejlich, Phys. Rev. A **56**, R2541 (1997).
[5] E. V. Podivilov, B. I. Sturman, S. G. Odoulov, S. Pavlyuk, K. V. Shcherbin, V. Ya. Gayvoronsky, K. H. Ringhofer, and V. P. Kamenov, Phys. Rev. A **63**, 053805 (2001).
[6] P. M. Garcia, A. A. Freschi, J. Frejlich, and E. Krätzig, Appl. Phys. B: Lasers Opt. **63**, 207 (1996).
[7] M. Gorkunov, B. Sturman, M. Luennemann, and K. Buse, Appl. Phys. B: Lasers Opt. **77**, 43 (2003).
[8] B. Sturman, E. Podivilov, and M. Gorkunov, Phys. Rev. E **72**, 016621 (2005).
[9] M. I. Rabinovich and D. I. Trubetskov, *Oscillations and Waves in Linear and Nonlinear Systems* (Kluwer Academic, Dordrecht, 1989).

[10] D. G. Luenberger, *Introduction to Dynamic Systems* (Wiley, New York, 1979).
[11] J. Bechhoefer, Rev. Mod. Phys. **77**, 783 (2005).
[12] S. A. Collins and K. C. Wasmundt, Opt. Eng. **19**, 478 (1980).
[13] S. I. Stepanov, I. A. Sokolov, G. S. Trofimov, V. I. Vlad, D. Popa, and I. Apostol, Opt. Lett. **15**, 1239 (1990).
[14] M. P. Petrov, I. A. Sokolov, S. I. Stepanov, and G. S. Trofimov, J. Appl. Phys. **68**, 2216 (1990).
[15] M. P. Petrov, S. I. Stepanov, and A. V. Khomenko, *Photorefractive Crystals in Coherent Optical Systems* (Springer-Verlag, Berlin, 1991).
[16] I. A. Sokolov and S. I. Stepanov, J. Opt. Soc. Am. B **10**, 1483 (1993).
[17] V. V. Bryksin, P. Kleinert, and M. P. Petrov, Fiz. Tverd. Tela (S.-Peterburg) **46**, 1566 (2004) [Phys. Solid State **46**, 1613 (2004)].
[18] Ph. Refregier, L. Solymar, H. Rajbenbach, and J. P. Huignard, J. Appl. Phys. **58**, 45 (1985).
[19] S. Mallick, B. Imbert, H. Ducollet, J. P. Herriau, and J. P. Huignard, J. Appl. Phys. **63**, 5660 (1988).
[20] T. E. McClelland, D. J. Webb, B. I. Sturman, E. Shamonina, M. Mann, and K. H. Ringhofer, Opt. Commun. **131**, 315 (1996).
[21] See, for example, http://www.analog.com/processors.